Improved PSO: A Comparative Study in MPPT Algorithm for PV System Control under Partial Shading Conditions

Wafa Hayder [1] , Emanuele Ogliari [2],*, Alberto Dolara [2], Aycha Abid [1], Mouna Ben Hamed [1] and Lasaad Sbita [1]

[1] Department of Electrical Engineering, National Engineering School of Gabes, 6029 Gabes, Tunisia; wafa.hayder@gmail.com (W.H.); aicha.abid@gmail.com (A.A.); benhamed2209@yahoo.fr (M.B.H.); lassaadsbita@yahoo.fr (L.S.)
[2] Department of Energy, Politecnico di Milano, 20156 Milan, Italy; alberto.dolara@polimi.it
*   Correspondence: emanuelegiovanni.ogliari@polimi.it; Tel.: +39-0223998524

Abstract: This paper deals with the implementation and analysis of a new maximum power point tracking (MPPT) control method, which is tested under variable climatic conditions. This new MPPT strategy has been created for photovoltaic systems based on Particle Swarm Optimization (PSO). The novel Improved Particle Swarm Optimization (IPSO) algorithm is tested in several simulations which have been implemented in view of the various system responses such as: voltage, current, and power. The performances of the proposed IPSO algorithm have been completed and compared with results of well-established methods adopted in the literature showing a higher accuracy.

1. Introduction

In recent years, solar energy has become one of the most popular renewable energy sources due to several advantages related to its availability and environmental sustainability [1–3]. Photovoltaic (PV) cells, as well as PV modules, strings, and arrays, are characterized by a nonlinear power–voltage (P–V) curve that depends on the incident irradiance, PV cells temperature [4,5] and, when they exist, partial shadings. One of the fundamental issues in PV generators is how to operate the generator at its maximum power point (MPP). Recently, a large number of research proposed different maximum power point tracking (MPPT) techniques. Traditional MPPT algorithms, such as power feedback, incremental conductance [6], short circuit current [7,8], open circuit voltage, ripple correlation control (RCC), and perturb and observe methods [9] require little hardware equipment and low computational burden. Nevertheless, they suffer of some drawbacks such as poor tracking accuracy, oscillations around the MPP, and/or long tracking time which reduces the system efficiency under rapidly changing environmental conditions. Several advanced MPPT techniques have been proposed to overcome these issues, as well as for tracking under various irradiance conditions and under partial shadings. They include methods based on Fuzzy Logic [5,10], Neural Network [11,12], Genetic Algorithms [13], and Particle Swarm Optimization (PSO) [14]. These MPPT algorithms differ in many features such as their complexity and the resulting computational burden, their steady state accuracy and efficiency, their range of effectiveness, their tracking speed, and their ability to track the MPP under changing environmental conditions and partial shading. PSO is a meta-heuristic algorithm and could be assigned to the group of optimization methods. The PSO algorithm was first implemented
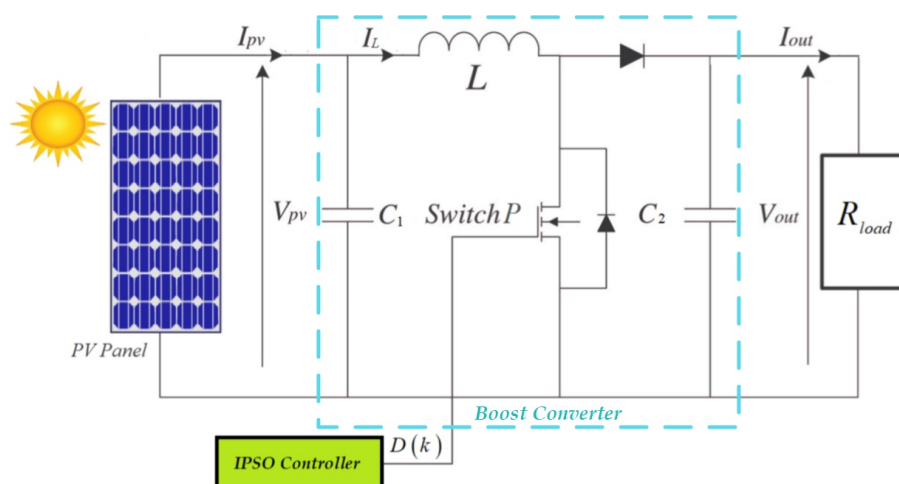
in a MPPT system by Miyateke et al. [15]. Authors have investigated the performance of the PSO algorithm under partial shading conditions, and the results show that PSO is capable of carrying out the global MPP search in the PV systems power output, under partial shading conditions. This is true only in the case that the partial shading has a very slow dynamic, that is, if the I-V characteristic does not change significantly during the global optimum research process [16].

The Improved Particle Swarm Optimization (IPSO) here proposed and implemented enhances the controller capabilities in the convergence speed and the MPPT detection accuracy when temperature and/or irradiation change. The enhancement of the PV system performance, in terms of convergence speed, stability, and accuracy, is based on the development of the controller algorithm. This controller process is responsible for computing the duty cycle value sending every sample time. Hence, the here proposed Improved Particle Swarm Optimization (IPSO) method is mainly affected by the determination of the correct duty cycle based on a mixed metric. This metric is able to converge the PV system towards the MPP under an environmental conditions change (especially shading conditions) and guarantee the highest accuracy. In addition, a comparison with the considered methods available in literature (ANN-PSO, P&O and GA) is presented.

The paper is organized as follows: Section 2 illustrates the modeling and the fundamental characteristics of the PV system used to test the proposed IPSO, Section 3 explains the IPSO algorithm, and Section 4 analyzes simulation results.

2. Characteristic of the Photovoltaic System

To validate the efficiency of generic IPSO algorithm, the modeling and programming of different PV system compositions: PV panel, IPSO controller, DC/DC boost converter and a resistive load are fundamental and they are associated as illustrated in Figure 1.

Figure 1. Electric scheme of the adopted photovoltaic (PV) system.

2.1. PV Module Modeling

The PV module taken into account in this work is the polycrystalline BP Solar MSX 120, whose ratings are reported in Table 1. This PV module consists of 72 polycrystalline silicon solar cells electrically arranged as four series strings of 18 cells, allowing three array configurations and the installation of bypass diodes on each 18-cell string. In this work, the 72-cell series configuration with 4 bypass diodes is taken into account.

The equivalent circuit of the PV cell is based on the five-parameter model, as shown in Figure 2, where I_{ph} represents the light-generated current, I_0 and n are the dark saturation current of the PN junction and the diode ideality factor, respectively [17,18], R_{sh} is the cell shunt resistance, and R_s is the cell series resistance.
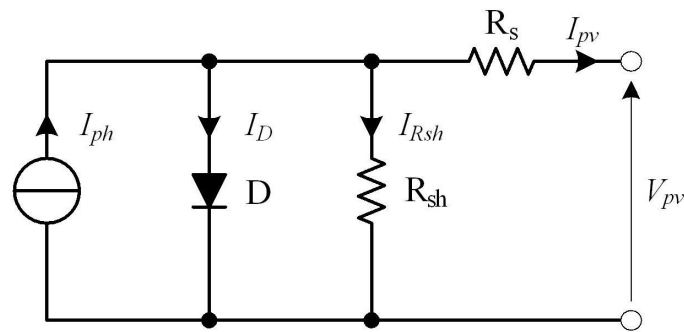
Figure 2. Five parameter equivalent model of a solar cell.

Hence, the I–V curve of the PV cell is defined by the following implicit equation:

$$I_{pv} = I_{ph} - I_0 \cdot \left(e^{\left(\frac{V_{pv} + I_{pv} \cdot R_s}{n \cdot V_t} \right)} - 1 \right) - \frac{V_{pv} + I_{pv} \cdot R_s}{R_{sh}} \tag{1}$$

V_t is the thermal voltage:

$$V_t = \frac{kT}{q} \tag{2}$$

where k is the Boltzmann's constant, q is the charge on the electron, and T is the PN junction temperature, which is the PV cell temperature T_c, in Kelvin. The light generated current depends on the irradiance, G, and the cell temperature as:

$$I_{ph}\left(G, T_c \right) = I_{ph,ref} \cdot \left(1 + \alpha_{Isc} \cdot \left(T_c - T_{ref} \right) \right) \cdot \frac{G}{G_{ref}} \tag{3}$$

where the subscript *ref* stands for reference conditions that usually are the Standard Test Conditions (STC) that are G_{ref} equal to 1000 W/m^2, cell temperature equal to 25 °C and Air Mass equal to 1.5. The reverse saturation current depends on the cell temperature as:

$$I_0\left(T_c \right) = I_{o,ref} \left(\frac{T_c}{T_{ref}} \right)^3 \cdot e^{\frac{E_g\left(T_{ref} \right)}{n \cdot k \cdot T_{ref}} - \frac{E_g\left(T_c \right)}{n \cdot k \cdot T_c}} \tag{4}$$

where E_g is the bandgap energy of the silicon that is in turn temperature dependent as:

$$E_g\left(T_c \right) = 1.17 - 4.73 \times 10^{-4} \cdot \frac{T_c{}^2}{T_c + 636} \tag{5}$$

The shunt resistance represents the whole set of mechanisms that can bring a photo-excited electron from the conduction band back to the valence band without flowing through the external circuit, mainly radiative recombination and recombination through defects. Hence, shunt resistance changes with solar radiation. The inversely proportional dependence of shunt resistance with irradiance is a good trade-off between simplicity and accuracy:

$$R_{sh}\left(G \right) = R_{sh,ref} \cdot \frac{G_{ref}}{G} \tag{6}$$

Ideality factor of the cell and the series resistance are considered not dependent on irradiance and cell temperature. The set of five values that characterize the equivalent circuit in the reference conditions are calculated from the PV module ratings (reported in Table 1) following the methodology described in [19]; the results are reported in Table 2. The I–V curve of each PV cell into the module is calculated according to Equations (1)–(6) for a given pair of incident irradiance and cell temperature.

Then, the PV module I–V curve is calculated combining the I–V curves of each cell and the I–V curves of each bypass diode in order to comply with the series and parallel electrical connection constraints.

Table 1. BP MSX-120 datasheet parameters.

Maximum power	P_{mp}	120 W
Voltage at P_{mp}	V_{mp}	33.7 V
Current at P_{mp}	I_{mp}	3.56 A
Short circuit	I_{scSTC}	3.87 A
Open circuit	V_{ocSTC}	42.1 V
Temperature coefficient of I_{scSTC}	α_{Isc}	0.065 %/°C
Temperature coefficient of V_{ocSTC}	β_{Voc}	−80 mV/ °C

Table 2. BPMSX-120 parameters.

Light-generated	$I_{ph,ref}$	3.8713 A
Diode saturation	$I_{0,ref}$	322.71 nA
Diode ideality	n	1.3976
Series resistance	R_s	0.4728 Ω
Shunt resistance	$R_{sh,ref}$	1365.8 Ω

In this paper, the most commonly used crystalline silicon PV module model has been adopted and simulations parameters are also those presented in the above-mentioned tables according to an existing manufactured PV module. However, the here proposed IPSO method is also valid for other PV modules' technologies as thin film and, more in general, in any case the here presented control algorithm should be calibrated for the peculiarities of the chosen type of PV module. Finally, the temperature effect could be added in the simulations, by matching the thermal model with the electrical model and calculate the I–V (or P–V) curve as a function of the temperature determined by the thermal model. However, thermal time constants are usually longer than the time frame of the simulation made in the context of this paper, which aims to analyze the behavior of the control logic against sudden irradiation steps. Therefore, we neglected thermal behavior in the simulations presented here.

2.2. Modeling of DC–DC Boost Converter and Design

The average state space model of the boost converter connected to the PV module is represented by the following set of equations [20–23]:

$$
\begin{cases}
\frac{dV_{PV}}{dt} = \frac{1}{C_1}\left(I_{PV}\left(V_{PV}\right) - I_L\right) \\
\frac{dV_{out}}{dt} = \frac{1}{C_2}\left((1-D)\,I_L - \frac{V_{out}}{R_{load}}\right), \\
\frac{dI_L}{dt} = \frac{1}{L}\left(V_{PV} - (1-D)\,V_{out}\right)
\end{cases}
\tag{7}
$$

where I_{pv} is the PV module output current V_{pv} is the output voltage of the PV, as well as the DC/DC converter input voltage and the voltage across the capacitor C_1, I_L is the current through the inductor L and V_{out} is the voltage across the capacitor C_2, R_{load} is the resistance of the load. The DC–DC boost converter is controlled to achieve the MPP by adjusting its duty cycle D ($D \in \left[D_{\text{inf}}...D_{\text{sup}}\right]$). This is generated by an adequate MPPT controller that is a Particle Swarm Optimization (PSO) algorithm.

3. MPPT Controller Based on the PSO Algorithm

In order to properly track the MPP, the PSO algorithm is generated, developed, and integrated as a PV system controller.

3.1. Traditional PSO Method

The PSO algorithm, called cooperative particles, consists of solving the problem of nonlinear systems optimization using a group of Np particles $(P_i)_{2 \leq i \leq Np}$. This technique is based on five steps: [24–29]:

- Step 1: Randomize the position of each particle D_i using Equation (8):

$$D_i = \alpha, 1 \leq i \leq Np \tag{8}$$

  where α is a random number $[D_{inf}...D_{sup}]$
- Step 2: Each particle finds its local best position (D_{Pbesti}).
- Step 3: All particles should follow the global best position (D_{Gbest}).
- Step 4: Adjustment of each particle position using Equations (9) and (10):

$$\Delta D_i^{k+1} = w \times \Delta D_i^k + r_1 c_1 \left(D_{Pbesti} - D_i^k \right) + r_2 c_2 \left(D_{Gbest} - D_i^k \right) \tag{9}$$

$$D_i^{k+1} = D_i^k + \Delta D_i^{k+1} \tag{10}$$

  where D_i^{k+1} is the new particle position; D_i^k is the actual particle position, ΔD_i^{k+1} is the perturbation to apply at the actual position; ΔD_i^k is the perturbation in the previous iteration; ω is the inertia weight; r_1 and r_2 are random variables within [0,1]; c_1 is the cognitive coefficient; c_2 is the social coefficient; D_{Gbest} is the global best position of the leader swarm particle; $D_{Pbest,i}$ is the local best position of the ith-particle.
- Step 5: Repeat Steps 2, 3, and 4 until all particles positions converge to the D_{Gbest}.

3.2. Sensitivity Analysis of the PSO Parameters (w, α, β)

To adapt the PSO technique in MPPT field, the particle position Di is considered as a duty cycle and is the duty cycle step that is based on the weighted summation of three criteria. This metric is expressed as follows:

$$\Delta D_i^{k+1} = w \times \Delta D_i^k + \alpha \left(D_{Pbesti} - D_i^k \right) + \beta \left(D_{Gbest} - D_i^k \right) \tag{11}$$

where $w + \alpha + \beta = 1$. D_{Gbest} is the duty cycle which corresponds to the global best power, while D_{Pbesti} designed the duty cycle value of i-th particle, which corresponds to the local best power generated during k iteration.
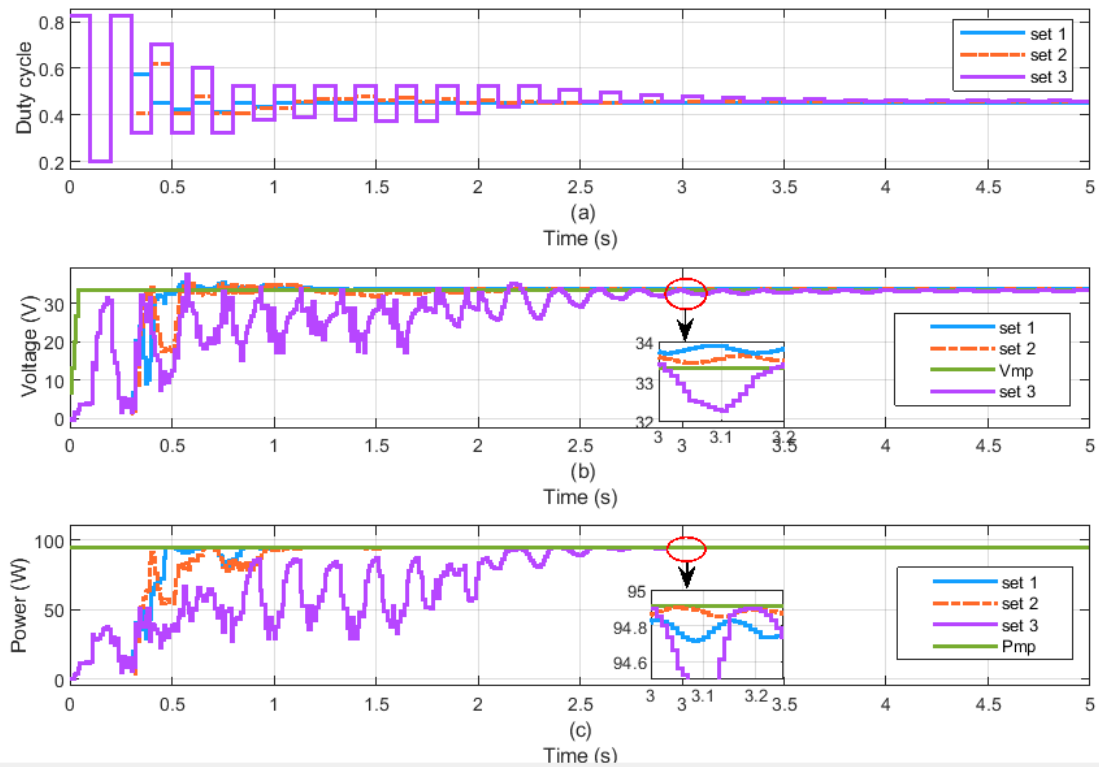
For example, if $w = 1$ ($\alpha = \beta = 0$), the duty cycle step (ΔD_i^{k+1}) never changes and it continues to increase or decrease until the maximum or the minimum limits $(D_{sup}$ or $D_{inf})$ of duty cycle are reached. It causes the PV system to never achieve the MPP.

In addition, if $\alpha = 1$ ($w = \beta = 0$), the new duty cycle value of particle i-th (D_i^{k+1}) converges to the local best duty cycle P_{besti}. This choice makes each particle insensitive to the global best position. Finally, if $\beta = 1$ ($\alpha = w = 0$), all particles converge to the first global best duty cycle D_{Gbest}.

The tuning of these three weighting coefficients results in different static and dynamic behaviour of the controller. A sensitivity analysis should be performed in order to assess the effectiveness of the three parameters mix. Three main scenarios are presented in Table 3 after the sensitivity analysis which was carried out. Before testing the PV system in different sets under constant environmental conditions (irradiance $G = 800$ W/m^2 and cell temperature $Tc = 25$ °C), under these conditions, the maximum power (P_{mp}) is 94.907 W, corresponding to a PV module voltage that is equal to 33.33 V. Figure 3 shows the simulation results obtained by using the sets of parameters reported in Table 3.

Table 3. Parameter values in different sets.

Set	w	α	β
1	0.2	0.2	0.6
2	0.34	0.33	0.33
3	0.2	0.6	0.2

Figure 3. Simulation results under different sets of parameters w, α and β given by PSO algorithm at constant irradiance and temperature (G = 800 W/m^2, T_c = 25 °C): (**a**) duty cycle, (**b**) voltage, and (**c**) power.

To evaluate the effectiveness and the efficiency that characterize the three sets of parameters w, α and β, two values are calculated: the accuracy in the steady state (A_{ss}) and the tracking energy losses (E_L) during a precise time interval [$t_0...t_n$]. These values are calculated by using Equations (12) and (13), respectively:

$$A_{ss} = \left(\frac{P_{ss}}{P_{mpp}} \right) \times 100 \tag{12}$$

$$E_L = \int_{t_0}^{t_n} \left| P_{mpp} - P\left(t\right) \right| dt \tag{13}$$

$$E_L\left(\%\right) = \frac{E_L}{E_{tot}} \tag{14}$$

where P_{ss} is the PV power in steady state, P_{mpp} is the power of the global maximum power point, and $E_L(\%)$ is the energy loss as the share of the overall energy computed in the time frame E_{tot}. To compare the PSO controller performances in the three sets of parameters, as shown in Table 4, the PV system controlled by PSO has been simulated for a time frame of 5 s, with t_0 = 0 s and t_n = 5 s.

Table 4. Comparison performances under different PSO parameters.

Set	Duty Cycle in the Steady State	V_{ss} (V)	P_{ss} (W)	E_L (%)	Transient Response (s)	A_{SS}
1	0.4508	33.6157	94.8639	6.70	0.9	99.95
2	0.4705	33.4519	94.9001	7.56	1.18	99.99
3	0.4514	33.3964	94.9020	19.19	3.81	99.99

It can be observed that set 1 is the fastest at achieving the steady state, but with the worst accuracy compared to other sets. The transient of PV output voltage, and consequently the transient of power, of set 1 has a small ripple and the less tracking losses due to its rapidity to achieve the steady state. On the other hand, the accuracy in the steady state is the lowest. These features are related to the high value of β, compared to the other two parameters. On the contrary, the parameters set 3 ensures the best steady state accuracy, almost equal to 100%, but the steady state is reached after a long transient response characterized by a lot of oscillations between the D_{Gbest} and D_{Pbesti}. A large scanning interval allows the system to search the optimum duty cycle that carries the PV system to the MPP. These features are related to the high value of α, compared to the other two parameters. A balanced metric, which corresponds to set 2, achieves a trade-off between time required to reach the steady state and steady state accuracy. Due to this metric, the duty cycle will be evolved with different steps and, after some iterations, the PV system converges to the MPP with acceptable rapidity and high precision.

3.3. Improved PSO Method

To guarantee the convergence of PV system towards the MPP regardless of environment conditions variations, the Improved PSO (IPSO) algorithm was created and presented in the following steps:

- Step 1:　Initialize Np, w, α, and β parameters.
- Step 2:　Initialize the k-th iteration and the index of the i-th particle at 1.
- Step 3:　If $k \leq Np$, the command which will be generated by the i-th particle is determined by applying Equation (8).
　　　　　If $k > Np$, the algorithm selected the i-th particle, which satisfies the following condition: the division remainder of (k-i) by Np is equal to 0, in order to complete the step and the new duty cycle D_i using Equations (9) and (10).
- Step 4:　Send the command $U = D_i$ to Boost converter. Measured the voltage V_{pv} and current I_{pv} to calculate the output power that corresponds to the i-th particle.
- Step 5:　The i-th particle must update its own best duty cycle which is designated D_{Pbesti}. Moreover, it is necessary to put a comparison between the best powers generated by Np particles during k iteration in order to update D_{Gbest} generated by the leader particle.
- Step 6:　If the convergence of each duty cycle produced by the particle i to D_{Gbest} is not reached yet, increase k by 1 and return to step 3.
　　　　　If D_{Gbest} is reached by all the particles that is to say $(D_{Pbesti})_{1 \leq i \leq Np} = D_{Gbest}$, then the converter must be operating in a regular way with this optimal duty cycle until a change in environmental conditions occurs which causes the return to step 2 for tracking the new MPP. These steps were summarized in the following flowchart (Figure 4):
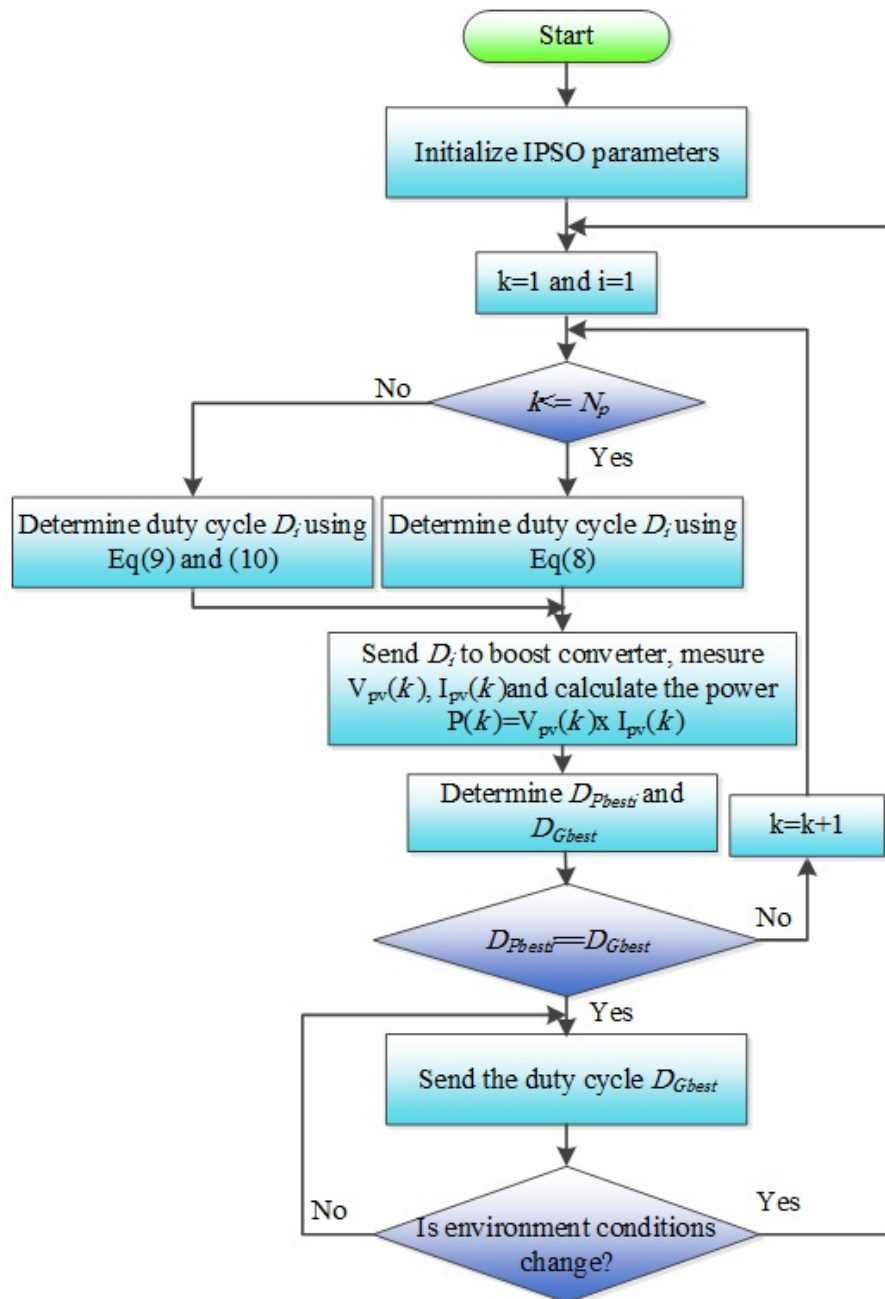
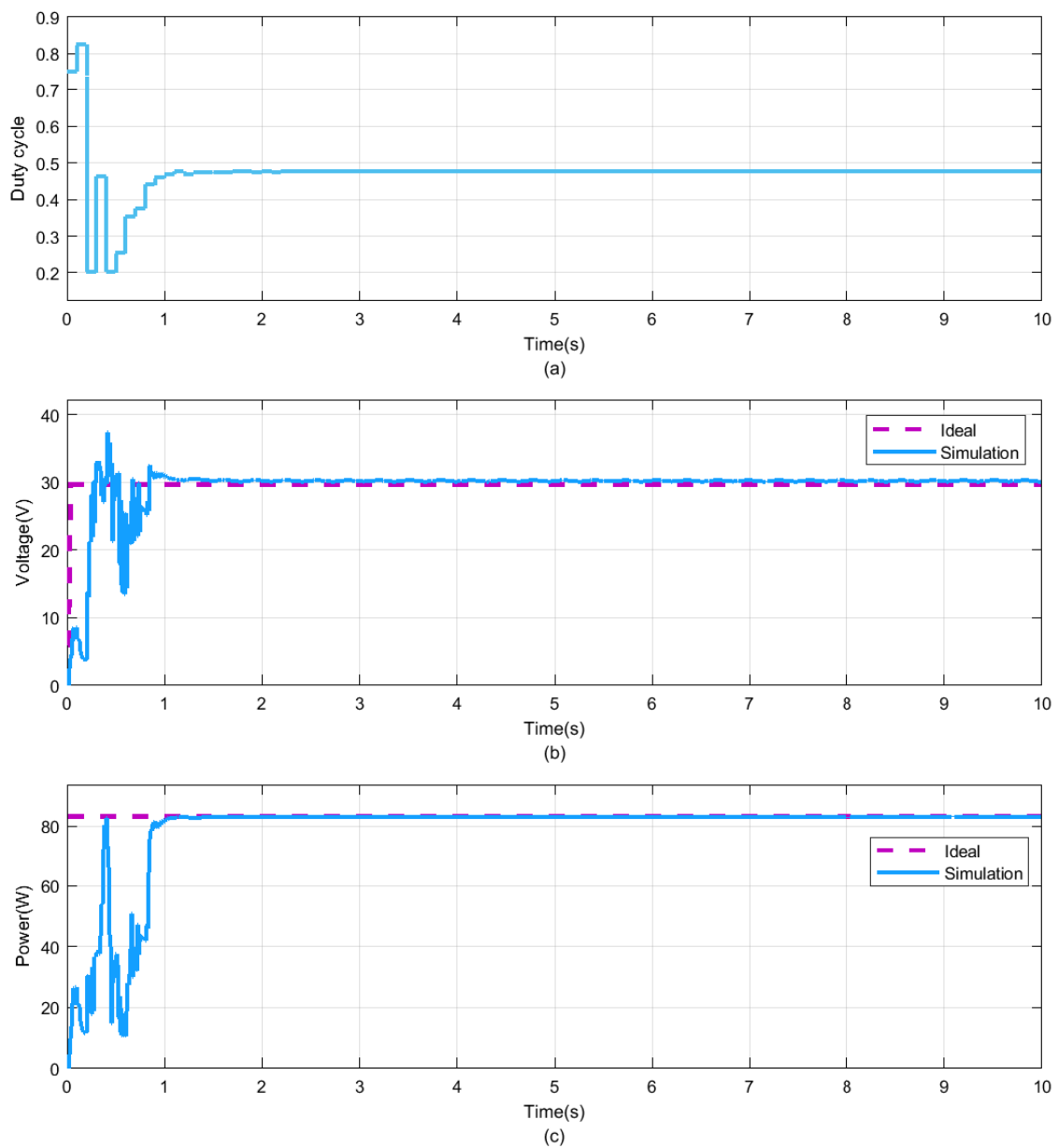**Figure 4.** Flowchart of the Improved Particle Swarm Optimisation (IPSO)-based MPPT algorithm.

4. Simulation Results under Different Environment Conditions

In order to highlight the IPSO method, different environmental conditions were adopted and applied on the PV system.
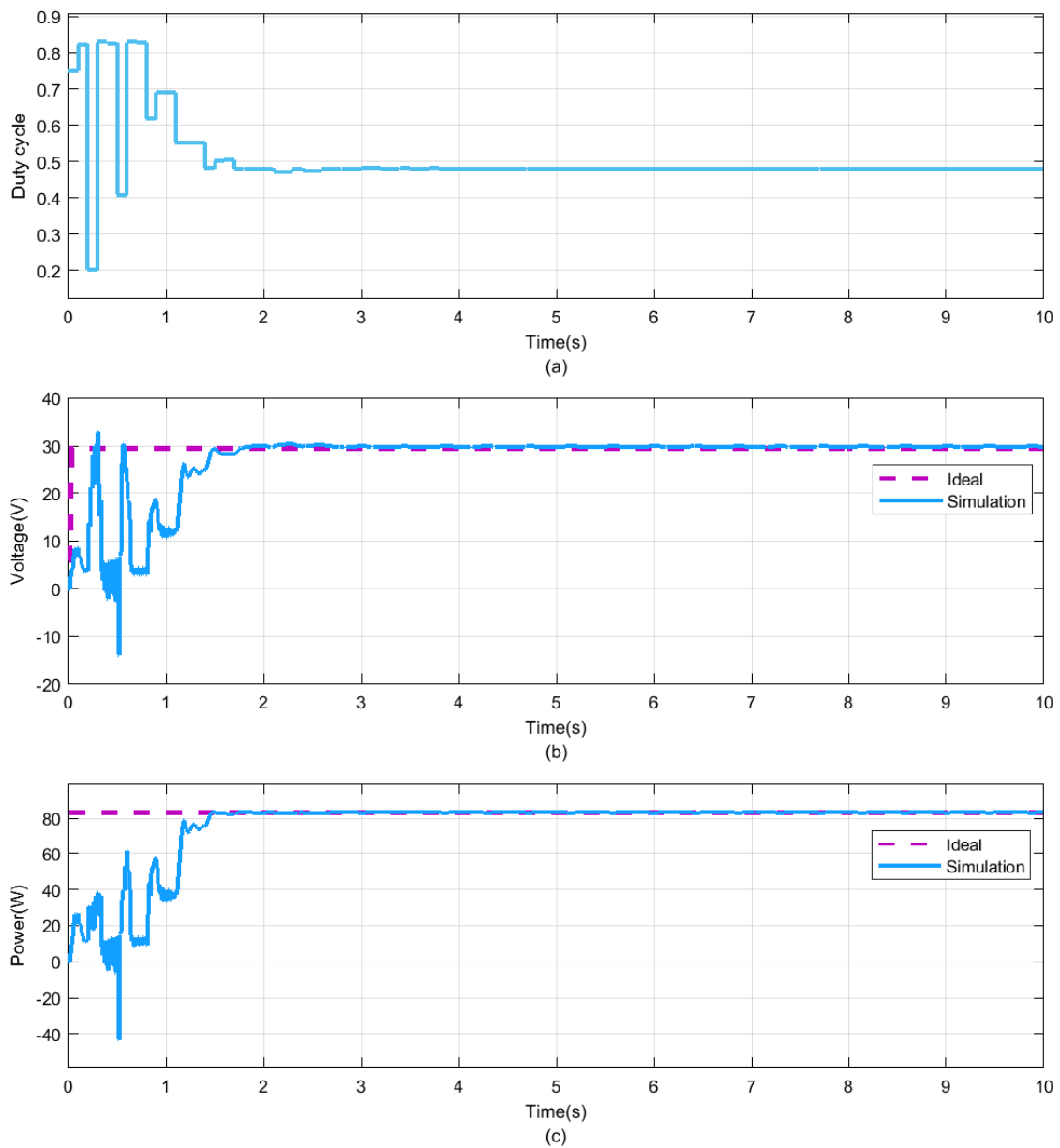
4.1. IPSO Method under Different Particles Number and Fixed Environment Conditions

To test the ability of IPSO algorithm for MPP reaching and know the effect of Np variation on performance satisfaction, a simple environment condition ($G = 800 \text{ W}/\text{m}^2$, $Tc = 48\,^\circ\text{C}$) was applied on the PV system. The simulations results are presented in Figures 5–8, which corresponds to $Np = 2$, $Np = 3$, $Np = 6$ and $Np = 10$, respectively.
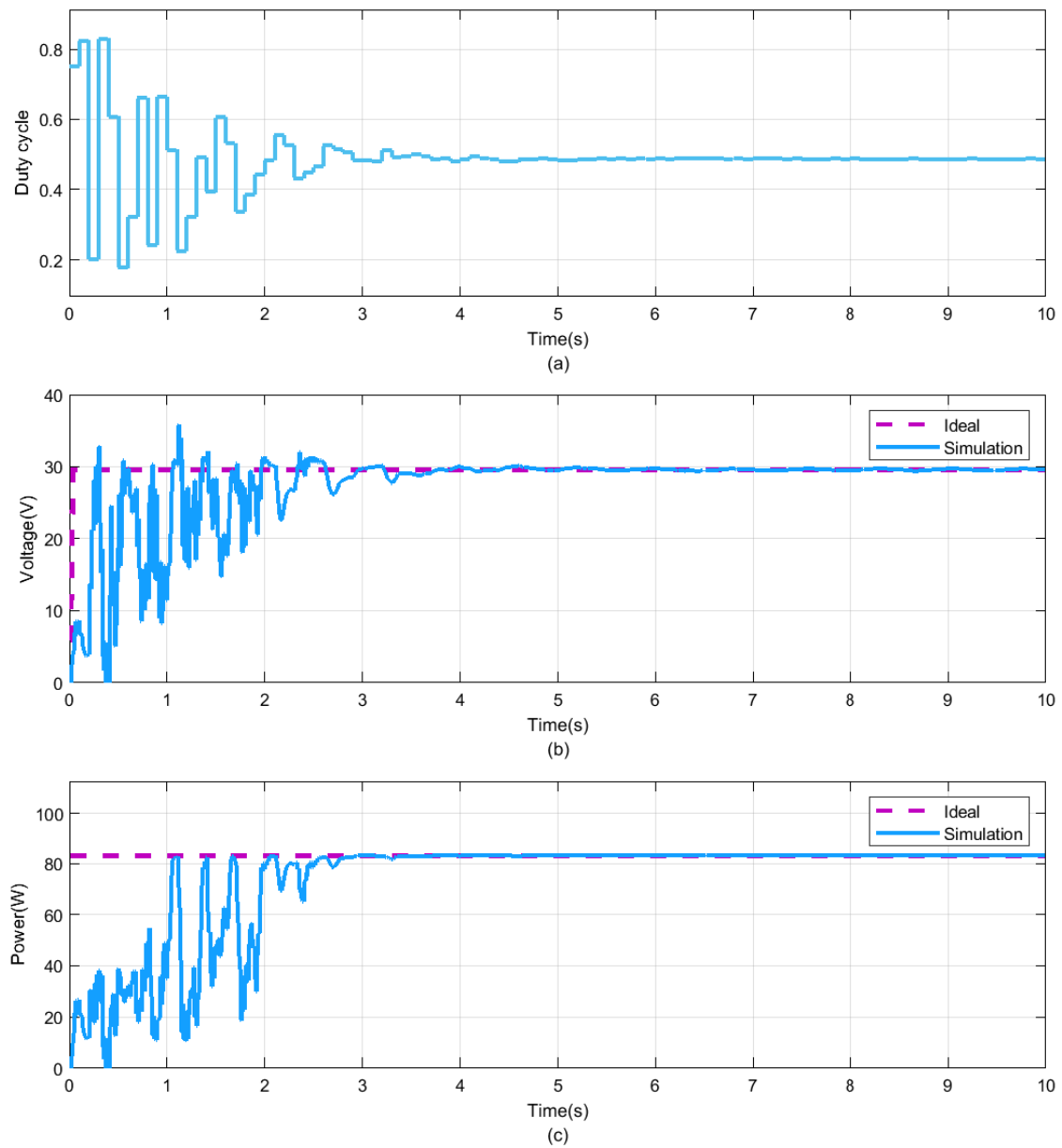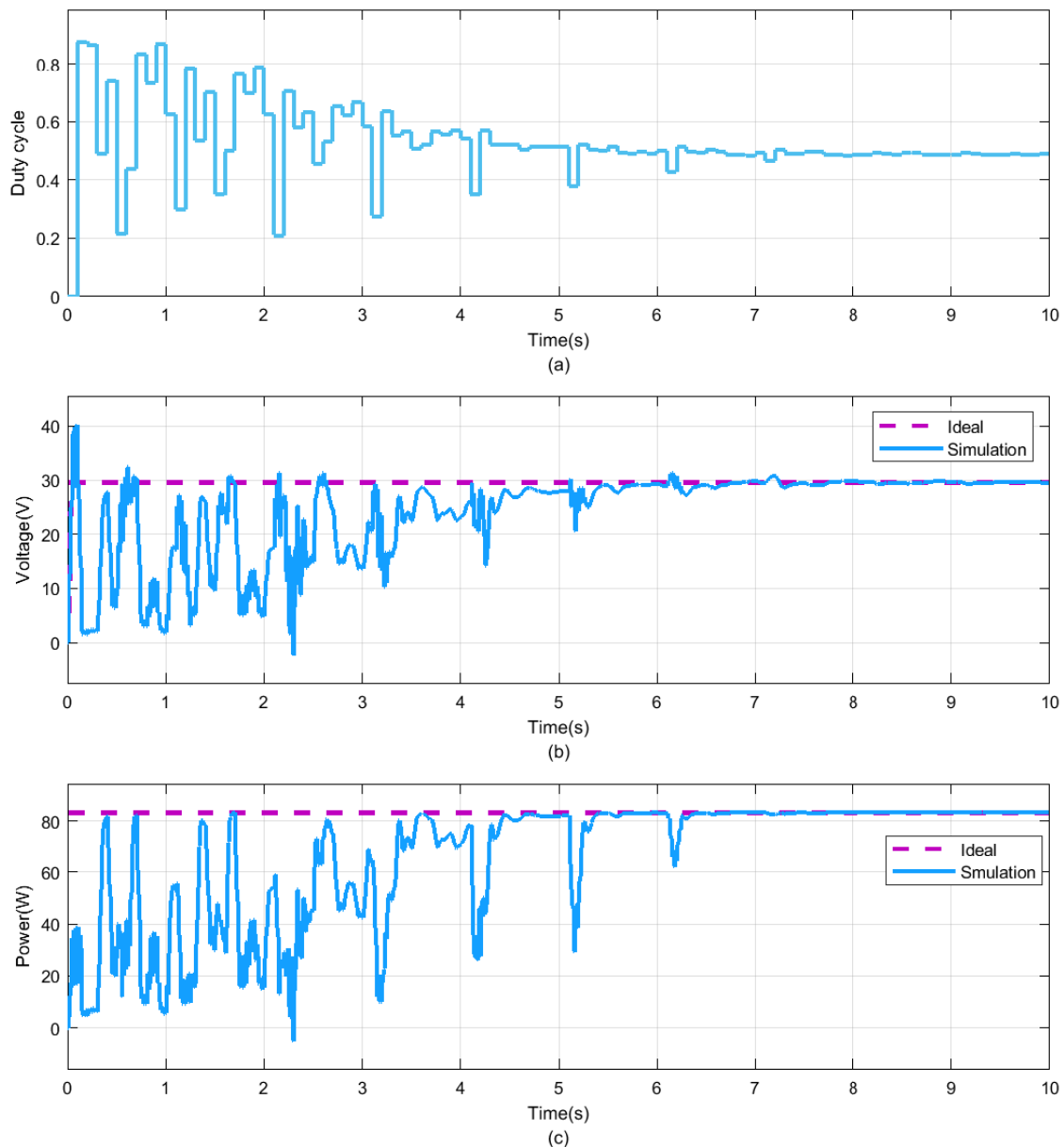
Figure 5. Simulation results under G = 800 W/m^2, Tc = 48 $^\circ$C and Np = 2 given by the Improved Particle Swarm Optimisation (IPSO) algorithm: (**a**) Duty cycle, (**b**) Voltage, and (**c**) Power.

Figure 6. Simulation results under G = 800 W/m^2, Tc = 48 $^\circ$C and Np = 3 given by the Improved Particle Swarm Optimisation (IPSO) algorithm: (**a**) Duty cycle, (**b**) Voltage, and (**c**) Power.

Figure 7. Simulation results under G = 800 W/m^2, Tc = 48 °C and Np = 6 given by the Improved Particle Swarm Optimisation (IPSO) algorithm: (**a**) Duty cycle, (**b**) Voltage, and (**c**) Power.

Figure 8. Simulation results under $G = 800$ W/m^2, $Tc = 48$ °C and $Np = 10$ given by the Improved Particle Swarm Optimisation (IPSO) algorithm: (**a**) Duty cycle, (**b**) Voltage, and (**c**) Power.

To be able to interpret the performance of Figures 5–8, a comparative table is generated. Table 5 shows that the precision when $Np = 3$ is more important than $Np = 2$, whereas, for the same interval time, the precision begins to decline when Np becomes greater than 3. It is remarkable also that the tracking losses energy grow when the Np increase due to the alternation between particle decisions, while the transient response for $Np = 3$ is smaller than $Np = 2$, and it increases beyond $Np = 3$. Hence, the existence of threshold Np value that must be completed to guarantee the best performances.

Table 5. Comparison performances under different Np values.

Np	Duty Cycle in the Steady State	V_{ss} (V)	P_{ss} (W)	E_L (%)	Transient Response (s)	A_{SS}
2	0.4759	30.0953	83.0623	10.75	1.77	99.84
3	0.4810	29.9190	83.1429	16.76	1.5	99.94
6	0.4869	29.6063	83.1905	22.60	2.97	99.99
10	0.4858	29.4027	83.1705	40.96	6.58	99.97

4.2. IPSO Method under a Series of Uniform Irradiation

In order to assess the IPSO method, a comparison with different methods that were found in literature [30,31], is presented. Therefore, the IPSO method was tested under a steep variation of the irradiance conditions, which is distributed over four intervals, while keeping the constant temperature equal to 25 °C as indicated in Figure 9 which are the same conditions found in literature [30,31]. This distribution is just an example which allows for knowing the robustness of the IPSO method and make a comparison with other works.
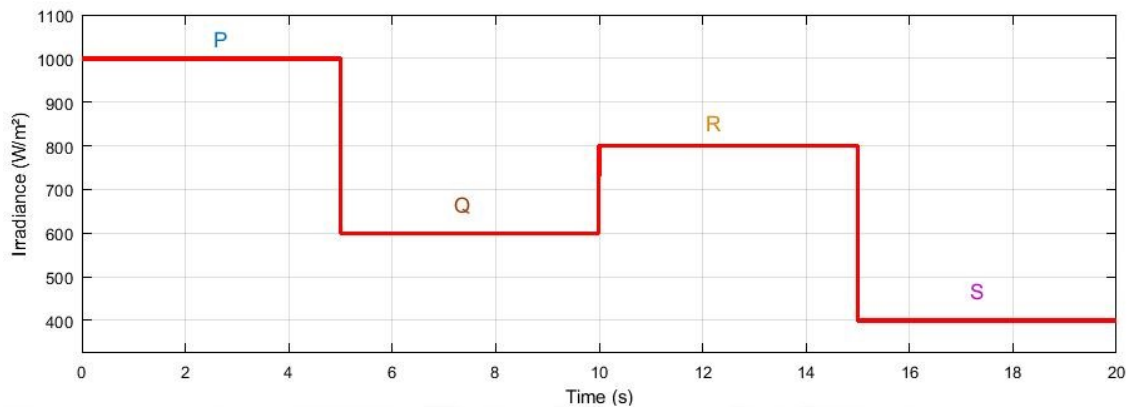

Figure 9. Irradiance profile of the whole panel without shading.

A series of simulations has been carried out with a different number of particles (Np) that will be defined when the error between the power resulting from G_{best} and the maximum power (P_{mpp}) tends towards 0. In Figure 10, the maximum power (P_{mpp}) and the optimal voltage (V_{mpp}) were determined after the simulation of the model under different values of irradiance which are showed in Table 6.
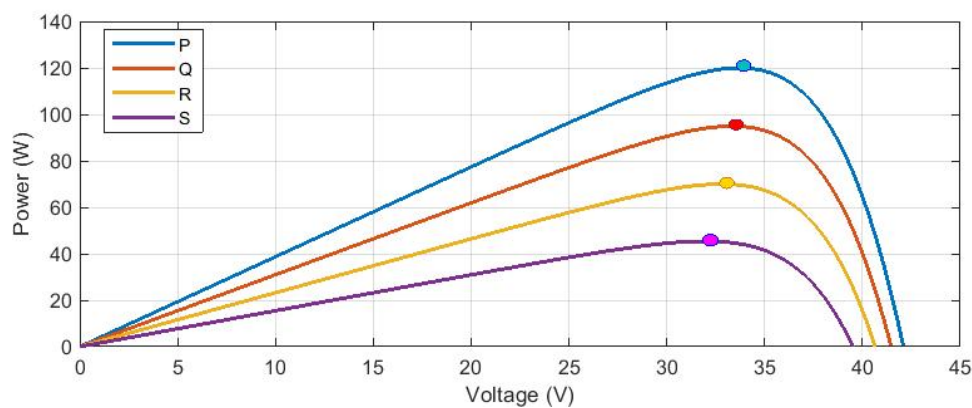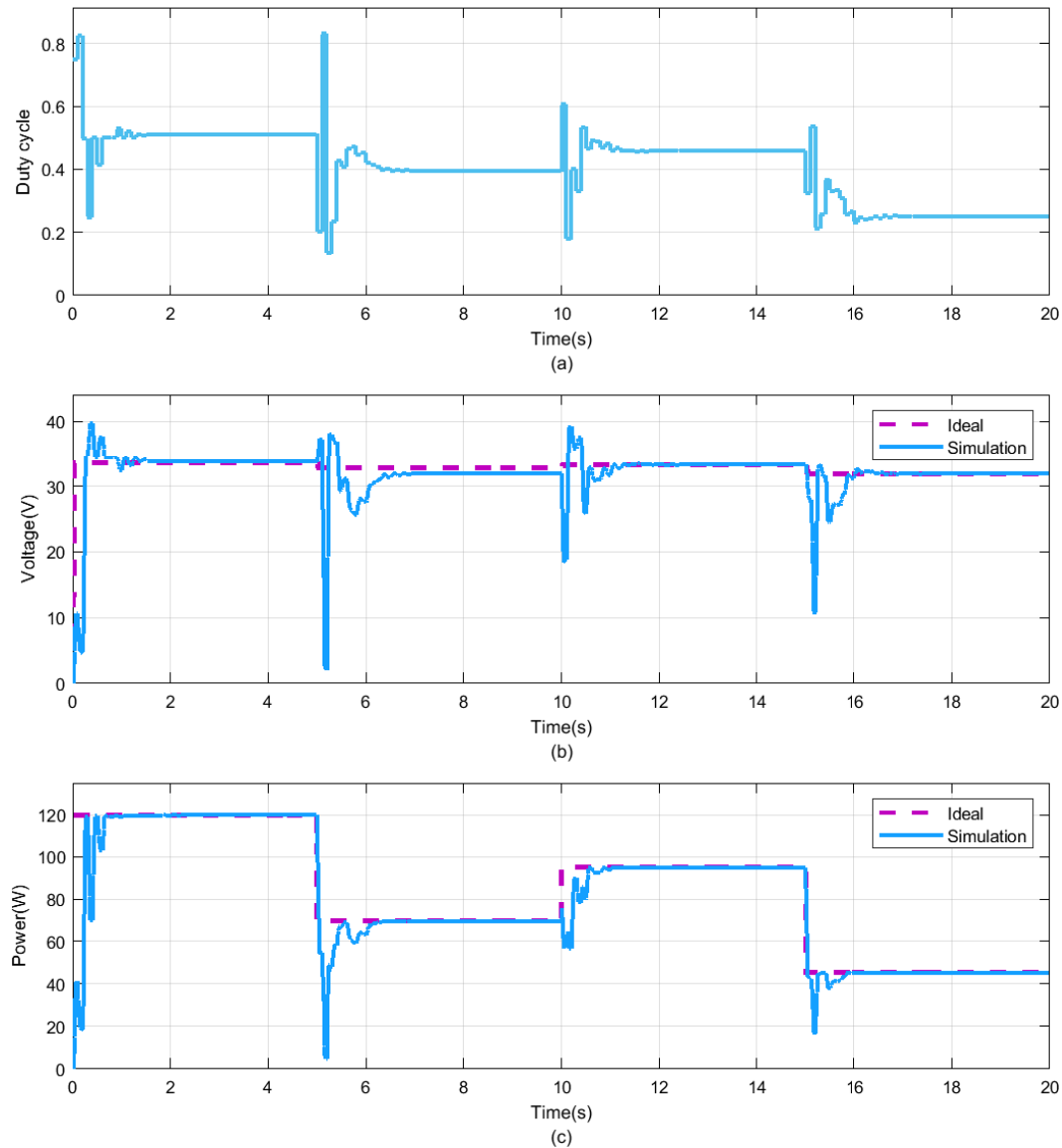

Figure 10. P–V curves of the photovoltaic (PV) panel affected by variable irradiance.

Table 6. MPPs for photovoltaic (PV) generator under different irradiance at 25 °C.

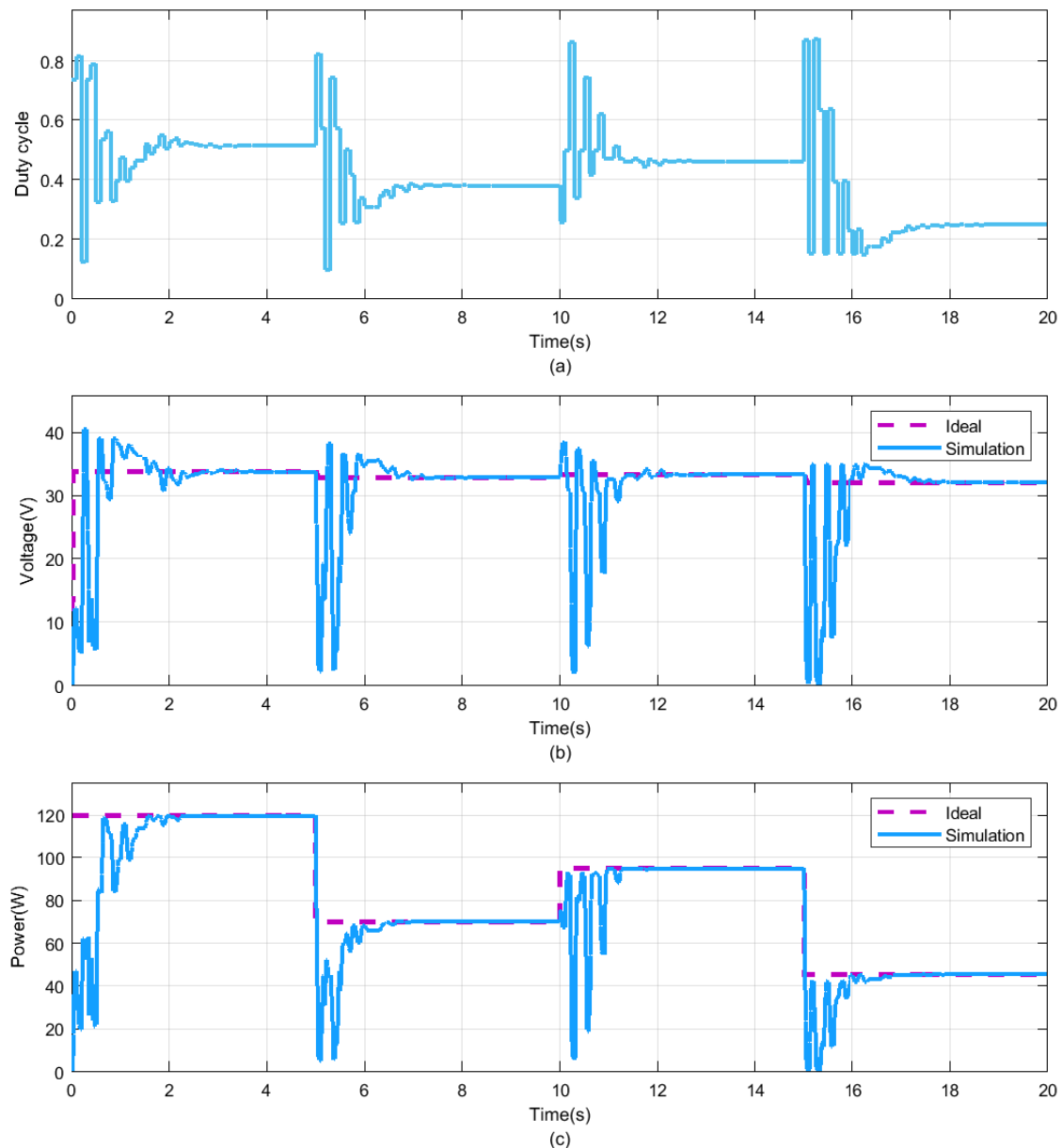| Set	Irradiance (W/m^2)	V_{mpp}	P_{mpp}
P	1000	33.70	119.9720
Q	600	32.79	69.9888
R	800	33.33	94.90
S	400	31.94	45.3924

In order to track the MPP using IPSO method, it is indispensable to choose the adequate number of particles Np. The simulation should be started using the minimum Np which is equal to 2 and then, if the performances such as rapidity and accuracy are not satisfied, the Np should be increased.

In this context, a PSO method based on 2 and 3 particles has been tested to verify the ability of the IPSO algorithm to track the MPP and to analyze the effects of increasing Np on transient duration, tracking losses, and steady state accuracy. The simulation results are presented in Figure 11 ($Np = 2$) and 12 ($Np = 3$).

Figure 11. Simulation results under irradiance variation and $Np = 2$ given by the Improved Particle Swarm Optimisation (IPSO) algorithm: (**a**) Duty cycle, (**b**) Voltage under irradiance change, and (**c**) Power under irradiance change.

Figures 11 and 12 show not only the ability of the IPSO algorithm to follow the MPP but especially the increase in accuracy when the particles number Np increases. Indeed, they approve that the IPSO method is able to follow MPP in all irradiation values and with different Np. Table 7 summarizes the results of the sensitive analysis concerning the number of particles, showing the steady state values of the duty cycle, the PV voltage (V_{ss}), the PV output power, and the response time (T_r) for each irradiance value (P, Q, R, and S).

Figure 12. Simulation results under radiation variation and $Np = 3$ given by the Improved Particle Swarm Optimisation (IPSO) algorithm: (**a**) Duty cycle, (**b**) Voltage under irradiance change, and (**c**) Power under irradiance change.

Table 7. Comparison performances of the proposed the Improved Particle Swarm Optimisation (IPSO) method when $Np = 2$ and $Np = 3$.

Np	Set	Duty Cycle	V_{ss} (V)	P_{ss} (W)	E_L (%)	Transient Duration (s)	A_{SS} (%)
$Np = 2$	P	0.5115	33.8109	119.9635	4.78	2.26	99.9929
	Q	0.3939	32.0184	69.7521	4.63	2.86	99.6618
	R	0.4589	33.3224	94.9072	2.42	1.85	99.9998
	S	0.2475	31.8400	45.3885	2.25	1.66	99.9914
$Np = 3$	P	0.5132	33.7030	119.9720	9.79	3.46	100
	Q	0.3795	32.7413	69.9874	7.15	2.36	99.9979
	R	0.4593	33.3393	94.9073	5.42	3.06	100
	S	0.2474	32.0115	45.3915	8.72	3.26	99.9980

Table 7 shows the effect of Np increasing on energy losses and accuracy. Thus, it is clear that, if the number of particles (Np) increases, the accuracy of the PV system response towards MPP grows, and the energy losses increases. In order to highlight the importance of the IPSO method based on a balanced metric, a comparison with other referenced methods, ANN-PSO [30] and PSO-P&O [31], is made and presented in Table 8. This is based on the calculation of accuracy between the power in the steady state (P_{ss}) and P_{mpp} for the same environmental conditions by applying Equation (12).

Table 8. Comparison accuracy between the Improved Particle Swarm Optimisation (IPSO), Neural Network (NN)-Particle Swarm Optimisation (PSO) [30], and PSO-Perturb & Observe (P&O) [31].

Algorithm	Set	P_{ss} (W)	P_{mpp} (W)	A_{SS} (%)
ANN-PSO [30]	P	669.1	897.3	74.57
	Q	665.7	723.2	92.05
	R	439.3	544.7	80.65
	S	302.1	362.5	83.34
PSO-P&O [31]	P	99.5	100.7	98.81
	Q	58.71	59.8	98.18
	R	79.42	80.7	98.41
	S	-	-	-
IPSO ($Np = 3$)	P	119.9720	119.9720	100
	Q	69.9874	69.9888	99.9979
	R	94.9073	94.9073	100
	S	45.3915	45.3924	99.9980

Table 8 presents an equitable comparison, between the results derived from the application of IPSO strategy and other methods used in literature and the same environment conditions [30,31]. From the two values of Power in the steady state and MPP in each set, the accuracy performance and the average precisions of different methods are calculated. It can be seen that the average accuracy of IPSO method based on balanced metric during the steady states is equal to 100%, while it is 82.65% with the ANN-PSO algorithm [30] and 98.47% for PSO-P&O [31]. Therefore, due to the integration of the mixed metric, exposed by Equation (11), IPSO becomes the best choice as it has the best performances in terms of simplicity and accuracy.

4.3. IPSO Method under Partial Shading

In order to test the robustness of IPSO technique, it is fundamental to analyze this method under partial shading conditions. Thus, a variable partially shade scenarios was adopted from [32]. The module's model (BP MSX-120 panel) adopted here includes four bypass diodes which means four substrings. The scenario of partially shading, used in this paper, needs two levels of irradiance affecting the substrings: the first is G and the second is designed by GS, which is defined in Equation (15):

$$GS = (1 - SI) \cdot G \tag{15}$$

where SI is the shading intensity. The partial shading GS affects the 25% of the panel area, as illustrated in Figure 13.
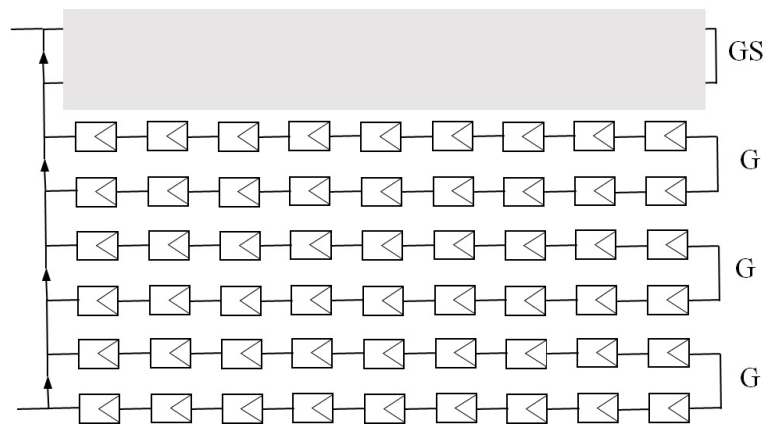
Figure 13. Shadow affecting 25% of the adopted panel area.

The changes in irradiance (*G*) and shading intensity (*SI*) were produced under four sets, as shown in Table 9 and Figure 14. The power voltage curve under partial shading conditions is characterized by multiple peaks; then, the controller has to make the differentiation between global MPP (GMPP) and local MPP (LMPP), as shown in Figure 15.

To verify the effectiveness of the IPSO method to track the GMPPs, a simulation in the partially shaded scenarios defined in Table 9 has been performed using two and three particles, which corresponds to Figure 16 and Figure 17, respectively.

Table 9. Global MPP (GMPP) and local MPP (LMPP) for photovoltaic (PV)generator under different sets of partial shading at 25 °C.

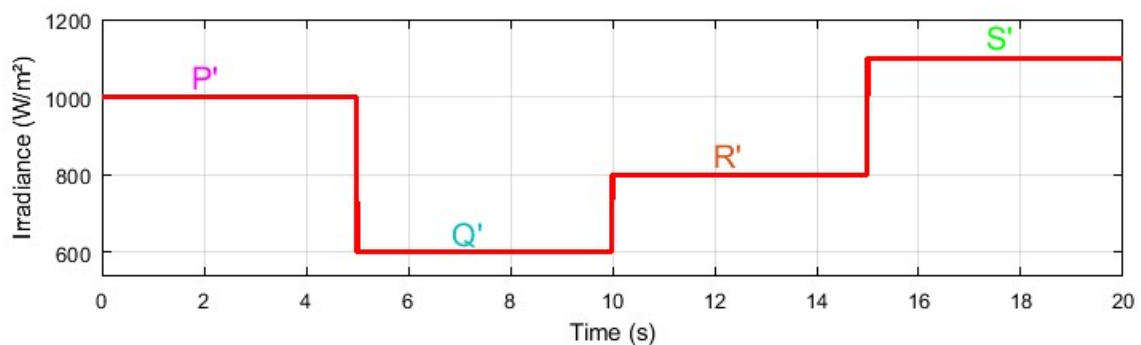| Set	Time (s)	G (W/m^2)	SI (%)	GS (W/m^2)	GMPP		LMPP	
					V_{mp}	P_{mp}	V_{LMPP}	P_{LMPP}
P′	[0,5]	1000	40	600	25.18	90.2943	37.75	56.89
Q′	[5,10]	600	0	600	25.18	55.2495	25.18	55.24
R′	[10,15]	800	25	600	25	73.0760	38.48	28.5
S′	[15,20]	1100	45.46	600	24.63	98.6604	37.36	70.69

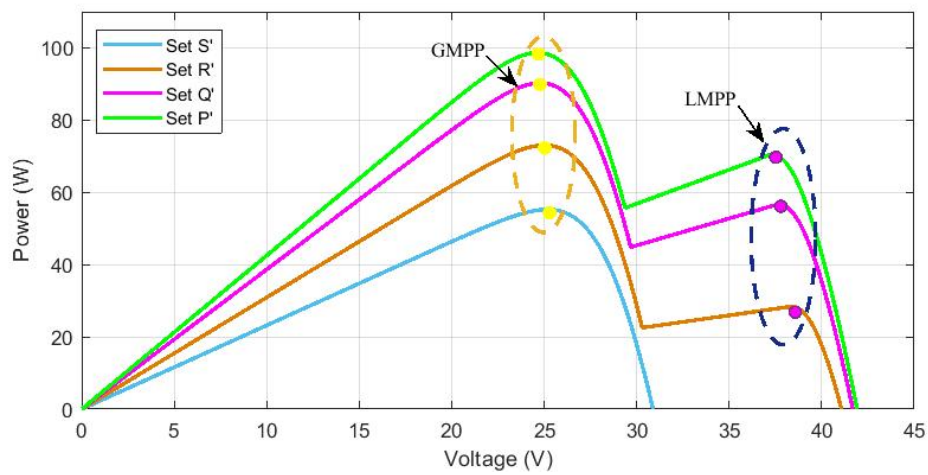**Figure 14.** irradiance values affecting 75% of the panel.

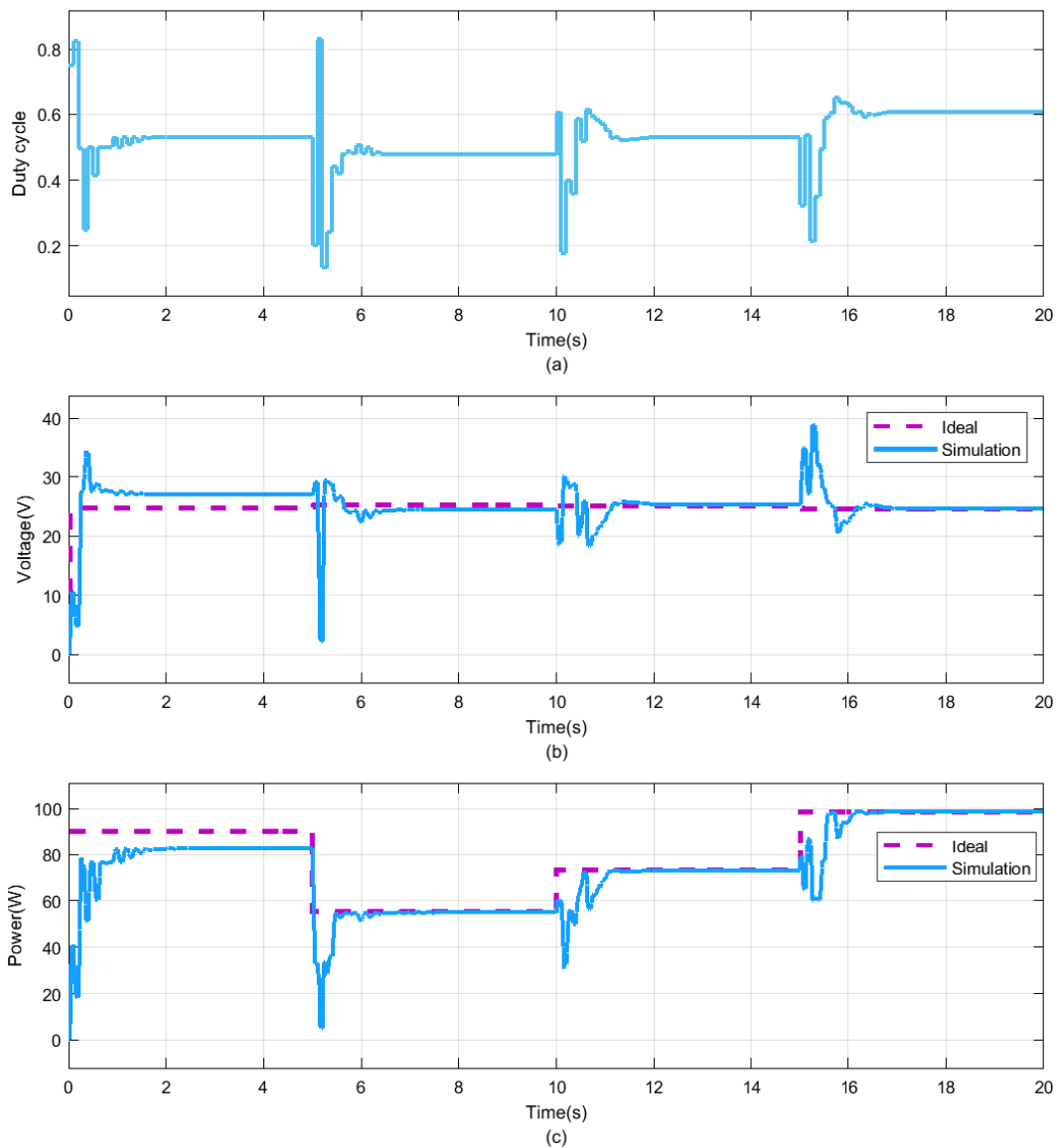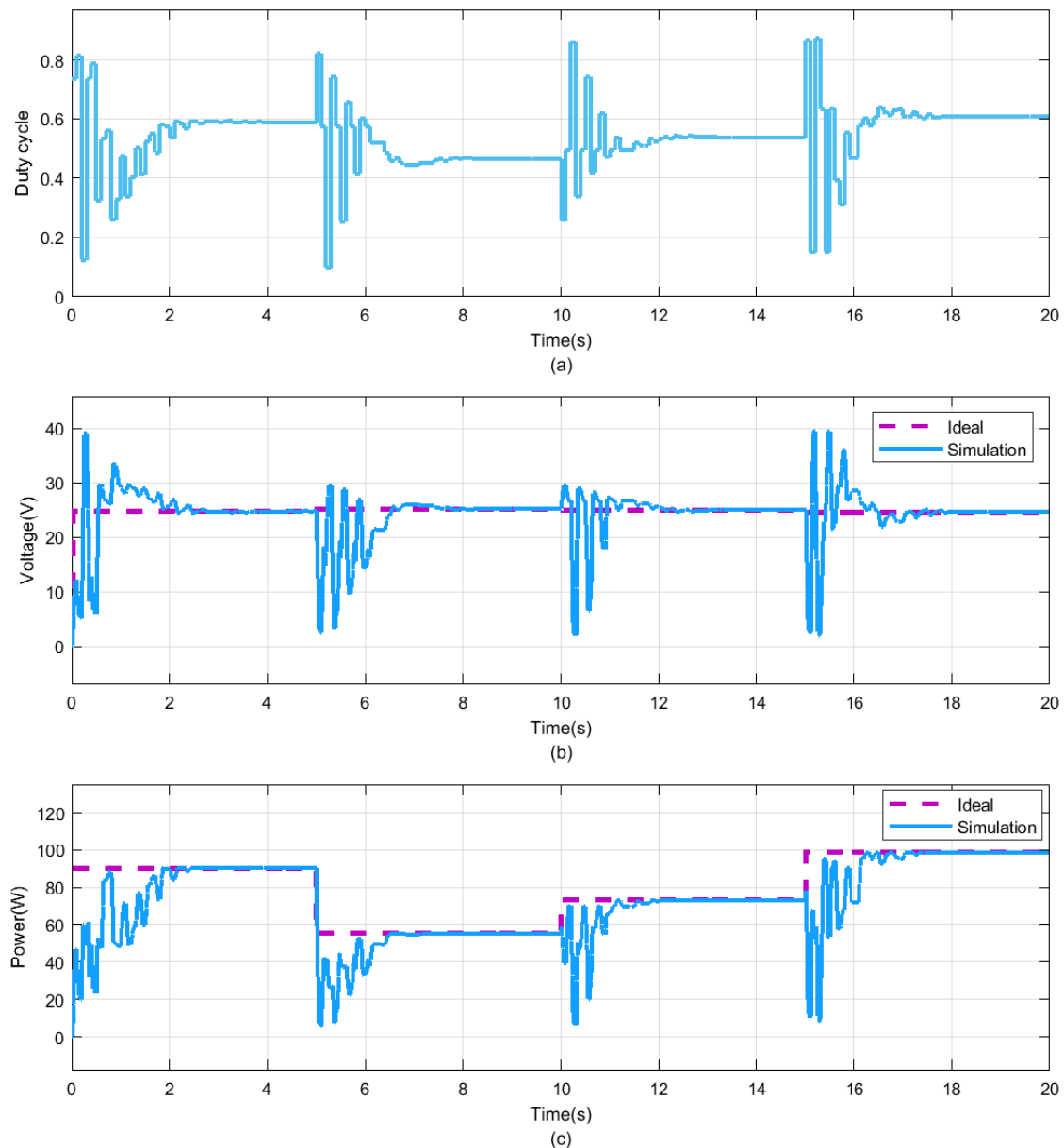**Figure 15.** P–V characteristics in different sets of partially shading.

Figure 16. Simulation results under different sets of partially shading and $Np = 2$ given by the Improved Particle Swarm Optimization (IPSO) method: (**a**) Duty cycle, (**b**) Voltage, and (**c**) Power.

Figure 17. Simulation results under different sets of partially shading and Np = 3 given by Improved Particle Swarm Optimization (IPSO) algorithm: (**a**) Duty cycle, (**b**) Voltage, and (**c**) Power.

The noticeable difference between Figures 16 and 17 is represented in the modification of accuracy values which occurred especially in the P' sets. Table 10 illustrated all parts of partially shading sets in terms of duty cycle, operating voltage, convergence power, energy losses, and transient response for two sets Np = 2 and Np = 3.

Table 10. Performance comparison of Improved Particle Swarm Optimization (IPSO) method under partial shading when $Np = 2$ and $Np = 3$.

Np	Set	Duty Cycle	V_{ss} (V)	P_{ss} (W)	E_L (%)	Transient Duration (s)
2	P′	0.5310	26.9670	82.6659	13.47	3.56
	Q′	0.4773	24.5042	54.9416	4.92	2.56
	R′	0.5310	25.3353	72.9674	4.12	2.66
	S′	0.6081	24.6476	98.6605	3.38	1.96
3	P′	0.5886	24.7296	90.2913	12.97	3.96
	Q′	0.4658	25.1612	55.2495	9.89	3.26
	R′	0.5380	25.0289	73.0759	6.43	3.26
	S′	0.6071	24.5797	98.6555	8.33	3.66

In fact, the passage from $Np = 2$ to $Np = 3$, provides the accuracy increasing. In order to highlight the IPSO technique related to other methods cited in [32] (PSO and Genetic Algorithm—GA), it is fundamental to calculate the accuracy using Equation (12) and complete Table 11.

Table 11. Accuracy comparison between techniques (Improved Particle Swarm Optimization (IPSO)) and (Particle Swarm Optimization (PSO), Genetic Algorithm(GA)) methods under partial shading.

Algorithm	Set	P_{ss} (W)	PGMPP (W)	A_{ss} (%)
PSO [32]	P′	237.5	239	99.4
	Q′	249.9	255.8	97.7
	R′	257.2	261.2	98.5
	S′	255.7	263.7	97
GA [32]	P′	230.8	239	96.6
	Q′	244.5	255.8	95.6
	R′	247	261.2	94.6
	S′	248.9	263.7	94.4
IPSO ($Np = 3$)	P′	90.2913	90.2943	99.99
	Q′	55.2495	55.2495	100
	R′	73.0759	73.0760	99.99
	S′	98.6555	98.6604	99.99

As it was shown for Table 8, it is noted that the average accuracy of IPSO technique during the steady states takes the high value compared to others methods in [32]. Therefore, due to the collaboration between the integration of the mixed metric of Equation (11), the proposed IPSO becomes the best choice. It has the best performances in terms of simplicity because it is based on a small number of particles and accuracy.

5. Conclusions

In this work, the new Improved Particle Swarm Optimization (IPSO) method was designed and implemented to track the maximum PV system power point for feeding the DC–DC boost converter. The method presented here is based on the search for the maximum point and therefore the algorithm performance (which are usually calculated on the convergence time and the steady-state error) strongly depends on the shape of the fitness function (which in our case is the P–V characteristic curve) and does not depend on the absolute values characterizing it. Given that, a partial shading completely changes the shape of the P–V curve, whereas the non-uniformity of the temperature in the PV module cells (those cells receiving less solar irradiation) causes a stretched P–V curve, but is not affecting its shape. Temperature effects and other noise sources have been neglected here and are currently under study. The sensitivity analysis in order to test the overall robustness of the presented algorithm is the subject of future work.

Hence, IPSO simulations performed under different irradiation conditions made the particles converge, according to consecutive iterations, to the leader swarm particle known by optimal duty cycle that moves the outputs' PV system to the maximum power point. Furthermore, the accuracy of the IPSO method is on average larger than 99%, even using a minimum number of particles, in comparison with the considered methods available in literature: ANN-PSO, P&O, and GA. Thus, the IPSO strategy is not only robust, but also it guarantees a higher efficiency of the PV system regardless of environment changing and partially shading.

References

1. Subudhi, B.; Pradhan, R. A Comparative Study on Maximum Power Point Tracking Techniques for Photovoltaic Power Systems. *IEEE Trans. Sustain. Energy* **2013**, *4*, 89–98. [CrossRef]
2. Ishaque, K.; Salam, Z. A review of maximum power point tracking techniques of PV system for uniform insolation and partial shading condition. *Renew. Sustain. Energy* **2013**, *19*, 475–488. [CrossRef]
3. Koutroulis, E.; Blaabjerg, F. A new technique for tracking the global maximum power point of PV arrays operating under partial-shading conditions. *IEEE J. Photovolt.* **2012**, *2*, 184–190. [CrossRef]
4. Villalva, M.; Gazoli, J.; Ruppert, E. Analysis and simulation of the P&O MPPT algorithm using alinearized array model. *Power Electron. Conf.* **2009**, 189–195. [CrossRef]
5. Al Nabulsi, A.; Dhaouadi, R. Efficiency optimization of a DSPbased standalone PV system using fuzzy logic and dual-MPPT control. *IEEE Trans. Ind. Inform.* **2012**, *8*, 573–584. [CrossRef]
6. Suwannatrai, P.; Liutanakul, P.; Wipasuramonton, P. Maximum power Point Tracking by Incremental Conductance Method For Photovoltaic System with Phase Shifted Full Bridge dc-dc Converter. In Proceedings of the 8th Electrical Engineering Electronics, Computer, Telecommunications and Information Technology (ECTI) Association of Thailand-Conference, Khon Kaen, Thailand, 17–19 May 2011.
7. Diaz, N.; Luna, A.; Duarte, O. Improved MPPT short-circuit current method by a fuzzy short-circuit current estimator. *IEEE Trans. Sustain. Energy Colomb.* **2011**, 211–218. [CrossRef]
8. Diaz, N.; Hernandez, J.; Duarte, O. Fuzzy MPP method improved by a short circuit current estimator, Applied to a grid- connected PV system. In Proceedings of the IEEE 12th Work Shop on Control and Modeling for Power Electronics, Boulder, CO, USA, 28–30 June 2010; pp. 1–6.
9. Femia, N.; Petrone, G.; Spagnuolo, G.; Vitelli, M. Optimization of perturb and observe maximum power point tracking method. *IEEE Trans. Power Electron.* **2005**, *4*, 963–973. [CrossRef]
10. Subiyanto, S.; Mohamed, A.; Hannan, M.A. Maximum Power Point Tracking in Grid Connected PV System using A Novel Fuzzy Logic Controller. *IEEE Stud. Conf. Res. Dev.* **2009**, 349–352. [CrossRef]
11. Syafaruddin; Karatepe, E.; Hiyama, T. Artificial neural network-polar coordi-nated fuzzy controller based maximum power point tracking control underpartially shaded conditions. *IET Renew. Power Gener.* **2009**, *3*, 239–253. [CrossRef]
12. Messalti, S.; Harrag, A.; Loukriz, A. A new variable step size neural networks MPPT controller: Review, simulation and hardware implementation. *Renew. Sustain. Energy* **2017**, *68*, 221–233. [CrossRef]
13. Larbes, C.; Cheikh, S.; Obeidi, T.; Zerguerras, A. Genetic algorithms optimized fuzzy logic control for the maximum power point tracking in photovoltaic system. *Renew. Energy* **2009**, *10*, 2093–2100. [CrossRef]
14. Cheng, Z.; Zhou, H.; Yang, H. Research on MPPT control of PV system based on PSO algorithm. In Proceedings of the 2010 Chinese Control and Decision Conference, Xuzhou, China, 26–28 May 2010; pp. 887–892.

15. Miyatake, M.; Veerachary, M.; Toriumi, F.; Fujii, N.; Ko, H. Maximum Power Point Tracking of Multiple Photovoltaic Arrays: A PSO Approach. *IEEE Trans. Aerosp. Electron. Syst.* **2011**, *47*, 367–380. [CrossRef]

16. Abdulkadir, M.; Yatim, A.H.; Yusuf, S.T. An improved PSO-based MPPT control strategy for photovoltaic systems. *Int. J. Photoenergy* **2014**. [CrossRef]

17. Sera, D.; Mathe, L.; Kerekes, T.; Teodorescu, R.; Rodriguez, P. A low-disturbance diagnostic function integrated in the PV arrays' MPPT algorithm. In Proceedings of the IECON 2011-37th Annual Conference on IEEE Industrial Electronics Society, Melbourne, Australia, 7–10 November 2011; pp. 2456–2460.

18. Dolara, A.; Grimaccia, F.; Mussetta, M.; Ogliari, E.; Leva, S. An evolutionary-based MPPT algorithm for photovoltaic systems under dynamic partial shading. *Appl. Sci.* **2018**, *8*, 558. [CrossRef]

19. Dolara, A.; Leva, S.; Manzolini, G. Comparison of different physical models for PV power output prediction. *Sol. Energy* **2015**, *119*, 83–99. [CrossRef]

20. Balamurugan, T.; Manoharan, S. Fuzzy Controller Design Using Soft Switching Boost Converter For MPPT in Hybrid System. *Int. J. Soft Comput. Eng.* **2012**.

21. Borle, L. Zero Average Current Error Control Methods for Bidirectional AC-DC Converters. Ph.D. Thesis, Electrical and Computer Engineering, Curtin University of Technology, Perth, Australia, 1999.

22. Blaabjerg, F.; Teodorescu, R.; Chen, Z.; Liserre, M. Power Converters and Control of Renewable Energy Systems. *Proc. ICPE* **2004**, 1–19. [CrossRef]

23. Erickson, R.W.; Maksimovic, D. *Introduction to Power Electronics, Fundamentals of Power Electronics*, 2nd ed.; Springer: Berlin/Heidelberg, Germany, 2001.

24. Ishaque, K.; Salam, Z.; Amjad, M.; Mekhilef, S. An improved particle swarm optimization (PSO)—Based MPPT for PV with reducedsteady-state oscillation. *IEEE Trans. Power Electron.* **2012**, *27*, 3627–3638. [CrossRef]

25. Soufi, Y.; Bechouat, M.; Kahla, S. Fuzzy-PSO controller design for maximum power point tracking in photovoltaic system. *Int. J. Hydrogen Energy* **2017**, *42*, 8680–8688. [CrossRef]

26. Sarvi, M.; Ahmadi, S.; Abdi, S. A PSO-based maximum power point tracking for photovoltaic systems under environmental and partially shaded conditions. *Prog. Photovolt. Res. Appl.* **2015**, *23*, 201–214. [CrossRef]

27. Qiang, F.; Nan, T. Complex-method-based PSO algorithm for the maximum power point tracking in photovoltaic system. In Proceedings of the 2010 Second International Conference on Information Technology and Computer Science (ITCS), Kiev, Ukraine, 24–25 July 2010; pp. 134–137.

28. Koad, R.B.A.; Zobaa, A.F.; El-Shahat, A. A Novel MPPT Algorithm Based on Particle Swarm Optimization for Photovoltaic Systems. *IEEE Trans. Sustain. Energy* **2017**, *8*, 468–476. [CrossRef]

29. Chaieb, H.; Sakly, A. Comparison between P&O and P.S.O methods based MPPT algorithm for photovoltaic systems. In Proceedings of the 2015 16th International Conference on Sciences and Techniques of Automatic Control and Computer Engineering (STA), Monastir, Tunisia, 21–23 December 2016; Volume 8, pp. 694–699.

30. Zakaria Said, S.; Thiaw, L. Performance of Artificial Neural Network and Particle Swarm Optimization Technique based Maximum Power Point Tracking for Photovoltaic System under Different Environmental Conditions. *J. Phys. Conf. Ser.* **2018**, *1049*, 012047, doi:10.1088/1742-6596/1049/1/012047. [CrossRef]

31. El-din, A.H.; Mekhamer, S.S.; El-helw, H.M. Comparison of Mppt Algorithms for Photovoltaic Systems Under Uniform Irriadiance Between Pso and P & O. *Int. J. Eng. Technol. Manag. Res.* **2017**, *4*, 68–77.

32. Badis, A.; Mansouri, M.N.; Sakly, A. PSO and GA-based maximum power point tracking for partially shaded photovoltaic systems. In Proceedings of the 2016 7th International Renewable Energy Congress (IREC), Hammamet, Tunisia, 22–24 March 2016; pp. 1–6.